Equivalence between free-electron-laser oscillators and actively-mode-locked lasers: Detailed studies of temporal, spatiotemporal, and spectrotemporal dynamics

C. Bruni*

Laboratoire de l'Accélérateur Linéaire, Université Paris–Sud 11, Unité Mixte de Recherche No. 8607 associée au Centre National de la Recherche Scientifique, Bâtiment 200, Boîte Postale 34, F-91898 Orsay Cedex, France

T. Legrand, C. Szwaj, and S. Bielawski

Laboratoire de Physique des Lasers, Atomes et Molécules, Unité Mixte de Recherche No. 8523, associée au Centre National de la Recherche Scientifique, Centre d'Études et de Recherches Lasers et Applications, Fédération de Recherche No. 2416, associée au Centre National de la Recherche Scientifique, Université des Sciences et Technologies de Lille, Bât. P5, F-59655 Villeneuve d'Ascq Cedex, France

M. E. Couprie

Synchrotron SOLEIL, L'Orme des Merisiers, Saint-Aubin, Boîte Postale 34, F-91192 Gif-sur-Yvette, France

(Received 22 April 2010; revised manuscript received 24 October 2011; published 1 December 2011)

We show experimentally and numerically that free-electron-laser (FEL) oscillators behave in a very similar way to conventional actively-mode-locked lasers. This stems from the similar structures of their underlying Haus equations. A comparative study of the temporal evolutions of the pulse train shapes and spatiotemporal regimes is performed on a Nd:YVO_4 laser and a storage-ring free-electron laser. Furthermore, since direct observations of time-resolved pulse shapes and spectra are more accessible on free-electron lasers, the analogy also potentially enables one to investigate mode-locked laser dynamics using existing FEL facilities.

DOI: 10.1103/PhysRevA.84.063804 PACS number(s): 42.60.Fc, 42.55.−f, 05.45.−a, 41.60.Cr

I. INTRODUCTION

At first glance, free-electron lasers [1,2] and actively-mode-locked lasers appear to be different types of systems because of their very different underlying physics. Indeed, in the free-electron-laser (FEL) case, the amplification is based on the energy exchange between an electromagnetic field and relativistic electrons circulating in a periodic, permanent magnetic field. This greatly contrasts with the amplification processes in classical lasers, based on transitions between quantum levels.

In spite of these apparent differences, common points exist between FEL oscillators (i.e., possessing an optical cavity) [2–8] and actively-mode-locked lasers [9], as suggested by the analogy between their typical cavity designs (Fig. 1). In this paper we show that the similarities have significant consequences on their dynamical behaviors, in particular on their instabilities. Careful consideration of FEL theory indeed reveals that the dynamical equation for the field in a FEL oscillator [6,8,10] has a structure that is equivalent to the Haus master equation for mode locking [9,11–13], the differences being located essentially in the gain description. To check whether the differences are relevant or not from the dynamical point of view, we perform detailed numerical and experimental studies of the two systems.

The motivation of this comparison is to find whether knowledge of FEL oscillators and mode-locked lasers may be fruitfully exchanged. Indeed, studies of the two systems meet different types of technical limitations.

(i) Although actively-mode-locked lasers are relatively low-cost tabletop lasers, dynamical studies are difficult given the very fast time scales involved. Hence few direct studies of pulse dynamics have been reported.

(ii) Free-electron lasers are large-scale facilities with limited time access. However, the time scale involved in the dynamics is slower by several orders of magnitude. This provides information on mode locking, through direct experimental recording of the pulse evolution dynamics, and on the spectrum versus time.

Hence a dynamical equivalence between the two types of lasers may open the way to studies of mode-locking issues, in a direct manner, for FEL oscillators. Conversely, FEL issues may also be studied using conventional laser systems as FEL models.

In Sec. II we make explicit the links between the structures of the two model equations. Then, in Sec. III, we compare the dynamical behaviors (in particular, self-pulsing) of free-electron lasers and actively-mode-locked lasers, focusing on the temporal aspect (the evolution of the pulse energy versus time). Finally, in Sec. IV, the spectrotemporal and spatiotemporal dynamics of both lasers are confronted numerically.

II. ANALOGY BETWEEN MODELS

A. Haus equations for the pulse amplitude

In the case of free-electron lasers as well as actively-mode-locked lasers, the starting point of the modeling is usually a map describing the pulse-shape evolution at each cavity round-trip time. In both lasers, a usual simplification is the so-called one-dimensional (1D) approach, where the transverse distribution of light is assumed to be fixed. The validity of this approach is tricky to demonstrate. However, it appears to be valid in practice for lasers with a single transverse-mode operation. This explains the wide success of

*bruni@lal.in2p3.fr

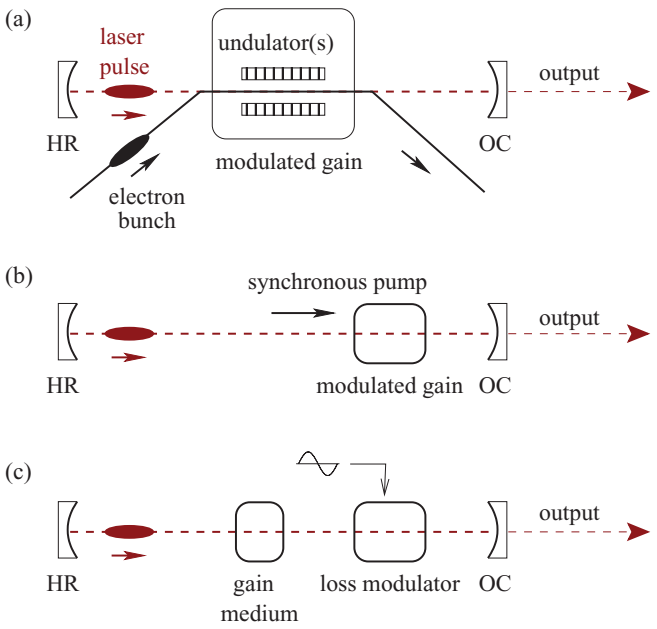

FIG. 1. (Color online) Paradigm of (a) free-electron-laser oscillators, (b) classical mode-locked lasers with a synchronous pump, and (c) classical mode-locked lasers with loss modulation. A main comparison point concerns the modulation of gain or losses at (or near) the round-trip frequency (or a multiple). HR denotes the high-reflection mirror and OC denotes the output coupler.

the 1D approaches of the Haus [9] and Dattoli-Elleaume [14] modeling. Thus, this 1D assumption will be also made here.

The well-known Haus master-equation approach leads to a simplification of the problem by taking the continuous limit of the map (see, e.g., Refs. [9,11,15] for classical lasers and Refs. [6,8,10,14,16] for FEL oscillators). As a consequence, the equation can be written with two independent times: a continuous slow time T, which corresponds to the number of round-trips in the cavity, and a fast time θ (at the picosecond or femtosecond scale), which resolves the pulses shape.

In FEL oscillators and actively-mode-locked lasers, the equations describing the evolution of the complex electric field $e(\theta,T)$ are very similar when written in dimensionless units. The evolution of the optical field in a FEL oscillator may be described by

$$e_T + v e_\theta = -e + g(T) f(\theta)[e - \alpha e_\theta + e_{\theta\theta}] + i D e_{\theta\theta} + \sqrt{\eta}\xi. \tag{1}$$

For loss-modulation active mode locking, the typical equation structure presents only slight differences from this FEL equation [see Eq. (1)] [9,11]:

$$e_T + v e_\theta = -e - \mu\theta^2 e + g(T)[e - \alpha e_\theta + e_{\theta\theta}] + i D e_{\theta\theta} + \sqrt{\eta}\xi. \tag{2}$$

In these models, T is expressed in units of the cavity field decay time τ_c and θ is expressed in units of a reference time scale t_U. In mode-locked lasers, assuming a Lorentzian gain shape, $t_U = \omega_C^{-1}$, with ω_C the full width at half maximum gain bandwidth. For the optical klystron [17] of an free-electron laser, $t_U = \omega_{OK}^{-1}\pi/\sqrt{2}$, with ω_{OK} being half the period of

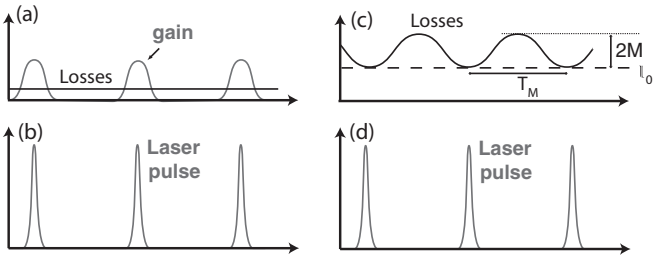

FIG. 2. Illustration of the temporal evolution of laser losses, gain, and intensity for (a) and (b) FEL oscillators (and, more generally, synchronously pumped lasers) and (c) and (d) loss-modulated mode-locked lasers.

the spectrum oscillation of the spontaneous emission. In mode-locked lasers, the values of t_U are from the picosecond range to a few femtoseconds, depending on the gain medium. In storage-ring free-electron lasers such as UVSOR [18] or ELETTRA [19], t_U is in the 100-fs range, $e(\theta,T)$ has periodic boundary conditions in θ, the period L is the cavity round-trip time in units of t_U, $f(\theta)$ is the temporal shape of the gain in FEL cases, and μ is a dimensionless parameter proportional to the loss modulation amplitude [9]:

$$\mu = \frac{1}{2}\frac{M}{l_0}\left(\frac{2\pi t_U}{T_m}\right)^2. \tag{3}$$

The definitions of l_0, M, and T_m are illustrated in Fig. 2: l_0 is the minimal round-trip intensity loss (i.e., the remaining loss in the absence of modulation), M is the amplitude of the round-trip intensity loss introduced by the modulator, and T_m is the modulation period, which is approximately equal to the cavity round-trip time in the case of our experiment. In addition, v characterizes the mismatch between the gain- (or loss-) modulation frequency ν_{RF} and the cavity round-trip frequency ν_R: $v = \frac{\nu_{RF}-\nu_R}{\nu_{RF}}\frac{\tau_c}{t_U}$. The term αe_θ accounts for the index of refraction induced by the amplifying medium. Typically α is $O(1)$, but it is usually neglected in free-electron lasers when the electron bunch is long with respect to t_U and in mode-locked lasers for which $\mu \ll 1$. This simplification ($\alpha = 0$) is also made here. Spontaneous emission is taken into account by the term $\sqrt{\eta}\xi$, with ξ a white-noise source of unit variance and η characterizing the level of noise. The term D characterizes the dispersion of the cavity, which is typically important for femtosecond lasers. In the long-pulse laser case considered here, dispersion is neglected. The equation terms have the same physical signification in the case of FEL oscillators and mode-locked lasers, though their derivations and naming occur in different ways. The diffusion term $e_{\theta\theta}$ accounts for the finite bandwidth. In the case of classical lasers, the derivation is performed phenomenologically, working in Fourier space [9]. For free-electron lasers, this is performed by taking into account the details of the interaction [14,20] and reflects the consequence of the so-called slippage effect [21]. The term e_θ on the right-hand sides of Eqs. (1) and (2) accounts for the decrease in light speed induced by the presence of gain. This corresponds to the change in refractive index due to the gain and is called lethargy in the case of free-electron lasers [22]. This term is typically neglected in the case where the laser pulse and/or the duration of $f(\theta)$

is much larger than t_U, as is the case here. Concerning the field equation, it initially seems natural to make a comparative study between free-electron lasers and synchronously pumped lasers because the equations for the field have very similar structures Eq. (1). However loss-modulated lasers, though having slightly different pulse field equations [Eq. (2)], are of interest in the present comparative study, where we will consider recirculation of the electron bunches in a storage ring. Indeed, in storage-ring free-electron lasers, the gain relaxation occurs at a very slow time scale with respect to the cavity lifetime and these free-electron lasers are thus class-B lasers [23] [linear accelerator (LINAC) free-electron lasers are synchronously pumped class-A lasers]. Since the relaxation time is a crucial point of laser dynamics and it is easier to achieve active mode locking of class-B lasers through loss modulation, we thus prefer to compare storage-ring FEL oscillators to loss-modulated class-B lasers. The differences in detail of the modulation origin will require the parameter domain to be carefully chosen.

B. Equations for the gain

The gain dynamics is more dependent on the laser specificities. In the simplest models for four-level class-B lasers, the gain evolution $g(T)$ obeys the following equation [6,24]:

$$\frac{dg}{dT}(T) = \gamma\left(R - g(T) - g(T)\int_0^L |e(T,\theta)|^2 d\theta\right), \quad (4)$$

where R is the pump parameter (pump power in units of its value at threshold) and γ is the relaxation rate of the population inversion in units of the field cavity lifetime (γ is typically small in solid-state lasers). Typical values for rare-earth-doped crystal lasers are in the 10^{-2}–10^{-4} range.

In storage-ring FEL oscillators, the gain saturation process occurs via a heating, i.e., an increase in the energy spread of the electron bunch [1]. In one of the simplest forms, the longitudinal dependence of the gain is constant,

$$f(\theta) = \exp -\left(\frac{\theta^2}{2\sigma_b^2}\right), \quad (5)$$

with σ_b the rms duration of the electron bunch, and the gain depends on time through its dependence on the bunch energy spread: [6,24]),

$$g(T) = \frac{A}{\sigma(T)}\exp\left(\frac{-[\sigma^2(T)-1]}{2}\right), \quad (6)$$

where σ is the rms width of the energy distribution of the electrons, in units of t_U, and A is a dimensionless parameter equivalent to the pump parameter in classical lasers and represents approximately the round-trip gain at the bunch center, in units of the round-trip losses. The energy spread evolution is given by [24]

$$\frac{d\sigma^2}{dT}(T) = \frac{1}{T_s}\left(1 - \sigma^2(T) + \int_0^L |e(T,\theta)|^2 d\theta\right), \quad (7)$$

with T_s the synchrotron damping time in units of the cavity field decay time. The relaxation time for the gain T_s is much longer that the field cavity lifetime ($T_s \gg 1$). This confirms that storage-ring free-electron lasers can be considered as class-B lasers.

In the following we compare dynamical studies of FEL oscillators and mode-locked lasers. Numerical studies are performed using Eqs. (1), (6), and (7) for the free-electron laser and using Eqs. (2) and (4) for mode-locked lasers, with the parameters corresponding to a Nd:YVO_4 laser. Experimentally, an expected necessary condition for analogous behaviors to occur concerns the pumping rate. In the case of free-electron lasers, the net gain is obtained only during a small time window [Fig. 2(a)]. In loss-modulated mode-locked lasers, such a situation is achieved only close to threshold [Fig. 2(b)].

III. ANALOGY BETWEEN TEMPORAL DYNAMICS: SELF-PULSING INDUCED BY DETUNING

In this section we consider temporal dynamics in both lasers at a slow time scale, i.e., without consideration of the internal structure of the pulse. An essential ingredient is the slow time scale of the gain relaxation dynamics, i.e., the fact that we are considering class-B lasers. The main consequence is the occurrence of self-pulsing in both types of lasers, with signal shapes resembling Q-switched mode locking (though the mechanism is more subtle, as it involves hypersensitivity to noise [11]).

A. Numerical results

The Haus-type equations for actively-mode-locked lasers [see Eqs. (2) and (4)] are integrated with the Runge-Kutta method of order 2 with an additive noise term [25]. The partial derivative along the longitudinal coordinate θ is calculated with a pseudospectral method using the FFTW library [26] and the field module is integrated with a trapezoid method. In free-electron lasers, when the detuning is very close to zero ($v \approx 0$), the output is a regular train of pulses with almost constant energy [Fig. 3(b)]. When the detuning is increased beyond

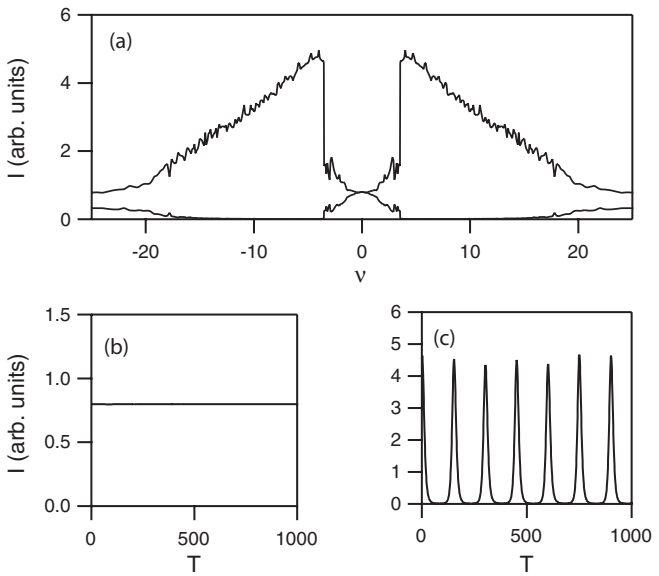

FIG. 3. (a) FEL detuning curve calculated from Eqs. (1), (6), and (7). For each value of v, the maxima and minima of the pulse energy $I = \int_0^L |e(T,\theta)|^2 d\theta$ are represented. Also shown is the intensity of the pulse train envelope for (b) $v = 0$ and (c) $v = 4.7$. The parameters are $A = 2$, $\sigma_b = 846$, and $\eta = 10^{-12}$.

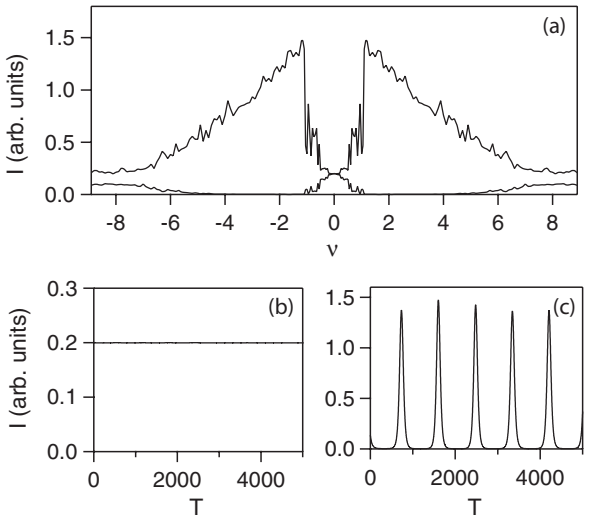

FIG. 4. Numerical results for the case of an actively-mode-locked laser. (a) Representation of the laser intensity as a function of the detuning parameter. Also shown is the laser intensity of the pulse train shape for (b) $v = 0$ and (c) $v = 1.15$. The normalized parameters used for the simulations are $R = 1.2$, $\gamma = 5 \times 10^{-4}$, $\mu = 5 \times 10^{-8}$, $D = 0$, and $\eta = 10^{-14}$.

a threshold, self-pulsing appears [Fig. 3(c)]. The bifurcation diagram representing the FEL output energy versus detuning v is well known and has a characteristic shape [4,5,27,28]. Figure 3(a) illustrates the typical detuning curve obtained from the integration of Eqs. (1) and (7).

Concerning this temporal dynamics, the similarity to actively-mode-locked lasers dynamics is particularly striking. Self-pulsing with a similar shape is also known to occur when the detuning parameter v is detuned from zero [see Fig. 4(c)]. Figure 4(a) depicts the bifurcation diagram versus detuning, obtained by integrating Eqs. (2) and (4).

B. Experimental results

To check this similarity in a more practical way, we realize and study experimentally an actively-mode-locked laser (see Fig. 5) emitting at 1.06 μm. The active medium is a Nd:YVO_4 crystal pumped by a fiber-coupled diode laser (10 W at 808 nm). Loss modulation is achieved using an acousto-optic mode locker driven at 50 MHz (i.e., with a 100-MHz modulation frequency). We place the output mirror on a motorized translation stage to study the dynamical behavior versus cavity length (and thus versus the detuning parameter v). The cavity round-trip time could be adjusted around 100 MHz. The output pulse dynamics is monitored using a fast photodiode resolving the individual mode-locked pulses (with a 1-ns response time) and a slower detector (with a 1-MHz response time) for monitoring the information related to the envelope of the mode-locked pulses.

Typical experimental results for the mode-locked laser near threshold are presented in Fig. 6. The observed dynamical behavior is very similar to the FEL case (see Fig. 3) and is consistent with numerical simulations presented in Fig. 4. Around perfect tuning [see Fig. 6(b)], we retrieve the stationary pulse-shape behavior observed in storage-ring free-electron lasers [see Fig. 3(b)]. At higher detuning values, the laser

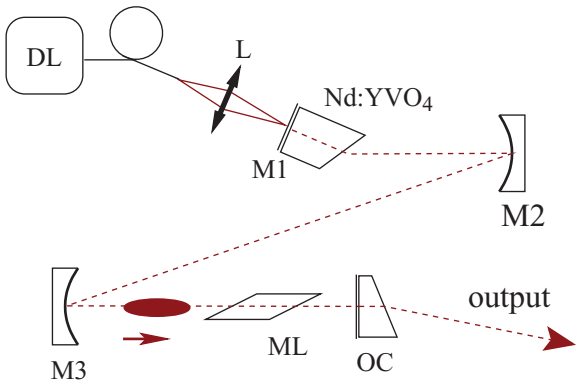

FIG. 5. (Color online) Experimental setup for the actively-mode-locked laser. A Nd:YVO_4 laser crystal (5 mm long) that is high-reflection coated at 1.06 μm on the pump side ($M1$) and Brewster cut on the other side is shown. DL denotes the diode laser (Thales TH-C1610-F2), 10 W at 808 nm, fiber coupled (with a diameter of 200 μm and a numerical aperture of 0.22); L denotes the aspheric lens; $M2$ and $M3$ denote high-reflection mirrors at 1.06 μm (with a radius of curvature of 50 and 20 cm, respectively); ML denotes the acousto-optic mode locker (IntraAction ML-503D1) with a Brewster-cut crystal; OC denotes the output coupler with a transmission of 5% and an antireflection face with a 3° wedge, mounted on a motorized translation stage.

pulse envelope presents strong oscillations [compare Figs. 6(c) and 3(c)].

To make a further comparison, we realize a detuning curve [see Fig. 6(a)] in conditions similar to the FEL case [see Fig. 3(a)]. For this purpose, the output mirror position (and thus the cavity length) is slowly swept using a motorized translation stage. Near threshold, the bifurcation diagram presents the characteristic shape of FEL detuning curves [29–33].

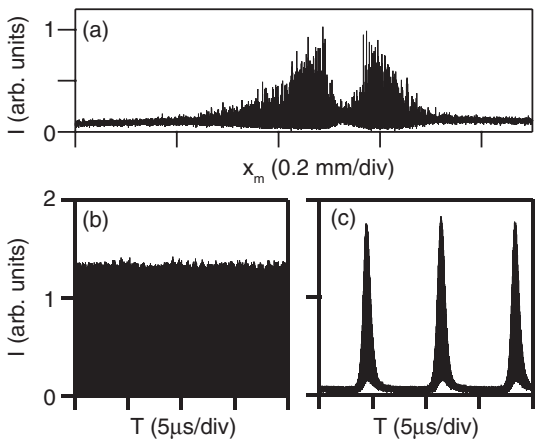

FIG. 6. (a) Experimental detuning curve versus cavity length in the actively-mode-locked laser. The laser power is measured with photodiode resolving the envelope variation, but not the individual pulses. (b) and (c) Time traces recorded with a detector resolving the individual pulses (the repetition rate is 100 MHz): (b) mode locking with a stationary envelope observed near perfect tuning ($v \approx 0$) and (c) mode locking with a pulsed envelope behavior observed at finite detuning [the mirror has moved approximately 0.05 mm from the (b) situation]. The experiment is performed near laser threshold ($R = 1.2$).

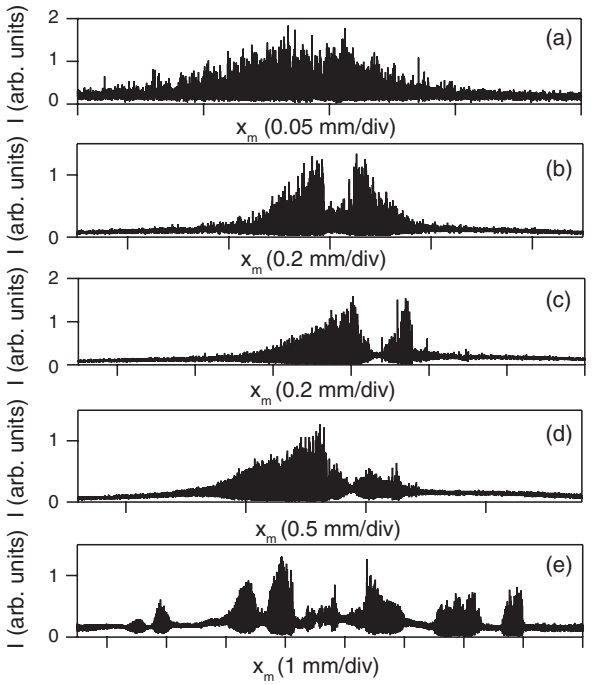

FIG. 7. Departure from the analogy between the free-electron laser and the mode-locked laser when the pump power is far above threshold. Detuning curves are recorded as in Fig. 6, versus pump power. The normalized pump power is (a) 1, (b) 1.1, (c) 1.3, (d) 1.7, and (e) 3.5.

Discrepancies appear at higher pump powers (see Fig. 7), confirming that FEL simulations using loss-modulated mode-locked lasers should be performed near the laser threshold.

Though the dynamics appears to be very similar, the time scales involved are drastically different. Typical self-pulsing frequencies are hundreds of hertz for FEL storage-ring oscillators and in the 140-kHz range for the present mode-locked laser. This is due to the differences in cavity lengths, cavity losses, and gain relaxation characteristic times. Indeed, compared to actively-mode-locked lasers, the cavity round-trip of free-electron lasers τ_R is typically one order of magnitude longer and cavity losses l are usually smaller. This leads to a much longer cavity damping time $\tau_c = \tau_R/l$. For a storage-ring free-electron laser, $l = 0.1\%$–1% and a cavity length larger than 10 m are typical. This leads to values for τ_c in the range of 10–100 μs, to be compared with the 100-ns range for the typical mode-locked laser used here ($\tau_R = 10$ ns and $l = 10\%$ round-trip losses). The characteristic time scale for the gain is also much longer for storage-ring free-electron lasers since T_s is typically in the range of tens of milliseconds.

Only the ratios between time scales are relevant for the dynamical behavior of the laser, as can be seen in the reduced equations [Eqs. (1), (2), (4), (6), and (7)]. However, it is important to note that practically, as we will see, the difference in time scales allows more detailed studies of the pulses dynamics to be performed in free-electron lasers.

C. Discussion

The similarity between the behavior of the FEL equations and that of the mode-locked laser equations suggests that the model differences are relatively unimportant. As conjectured,

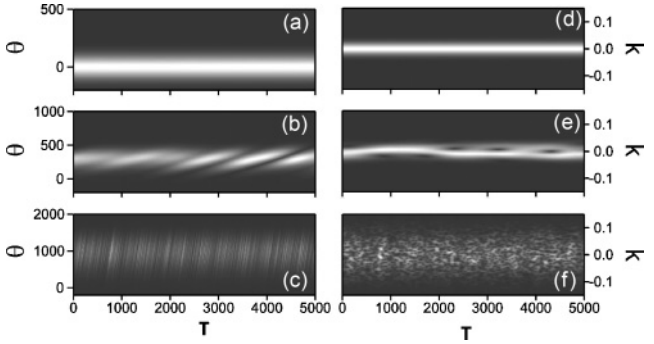

FIG. 8. Numerical results in the case of an actively-mode-locked laser. (a)–(c) Representation of the pulse intensity distribution (vertical scale) as a function of time (horizontal scale). (d)–(f) Representation of the pulse spectral distribution (vertical scale) as a function of time (horizontal scale). The normalized parameters used for the simulations are $R = 1.2$, $\gamma = 5 \times 10^{-4}$, $\mu = 5 \times 10^{-8}$, $D = 0$, and $\eta = 10^{-14}$ for different detuning values: (a) and (d) $v = 0$, (b) and (e) $v = 0.15$, and (c) and (f) $v = 8.8$.

differences in field equations (i.e., loss versus gain modulation) have minor consequences in the case in which the net gain is periodically positive and negative (i.e., when the mode-locked laser is close to threshold).

The differences in the gain dynamics initially seems more important. The similarities observed in the behavior can be attributed to the fact that the main ingredients are the same in both lasers: (i) Saturation of the gain depends on the pulse energy (global saturation coupling) and (ii) the time scale of the gain relaxation time is much longer that the field cavity lifetime (both are class-B lasers). For these reasons we may expect the qualitative behavior to be largely independent of the details of gain saturation while these two conditions are met.

IV. ANALOGY BETWEEN SPATIOTEMPORAL AND SPECTROTEMPORAL DYNAMICS

The model given by Eqs. (2) and (4) has been integrated and the spatiotemporal and spectrotemporal results are represented in Fig. 8. The behavior is similar to the FEL one. Above a certain detuning threshold, advection instabilities appear, leading to so-called optical turbulence [12,13]. These instabilities in the spatiotemporal space are associated with intensity holes in the spectrotemporal space [6]. The length of the spectrotemporal defects are on the order of 1 ms in the FEL case versus 1 μs in the actively-mode-locked laser one. This length depends on the characteristics times of the system being the relaxation time of the media and the photon lifetime in the cavity and the losses.

To explore the formation of pattern, lasers are particularly adapted. However, the very fast dynamics constitutes a major drawback. As a consequence, free-electron laser appears to be a better natural candidate to investigate the spatiotemporal dynamics from the point of view of a slower dynamics.

V. COMPARISON OF ULTIMATE PULSE DURATION AND TIME-BANDWIDTH PRODUCT

Both types of lasers appear to present a similar limitation in terms of pulse duration. In the case of classical mode-locked

lasers [9,11], it is well known that the stationary solution is typically a Gaussian pulse. Assuming $D = 0$, $\alpha = 0$, and $\eta = 0$, the fundamental stationary solution of Eq. (2) is (see Appendix B for details), for both lasers,

$$e_S(\theta) = a \exp\left(-\frac{\theta^2}{4\sigma_L^2}\right) \tag{8}$$

or in terms of the physical time t (in seconds),

$$e_S(t) = a \exp\left(-\frac{t^2}{4t_L^2}\right), \tag{9}$$

where a is the pulse amplitude. These expressions are valid when $\sigma_b \gg 1$. The dimensionless rms pulse duration σ_L and its associated physical rms pulse duration (in seconds) t_L are, respectively,

$$\sigma_L = 2^{-1/4}\sqrt{\sigma_b}, \tag{10}$$

$$t_L = 2^{-1/4}\sqrt{t_b t_U} \tag{11}$$

for the free-electron laser, where t_b is the bunch duration in physical units (in seconds) and

$$\sigma_L = \left(\frac{1}{4\mu}\right)^{1/4}, \tag{12}$$

$$t_L = \frac{1}{\sqrt{2\pi}}\left(\frac{l_0}{2M}\right)^{1/4}\sqrt{T_m t_U} \tag{13}$$

for the actively-mode-locked laser. In both cases, the field has a Gaussian shape. As a consequence, at perfect tuning, the minimum time-bandwidth product can be obtained (also known as the Fourier limit). This is well known for mode-locked lasers [9]. In the case of free-electron lasers, experiments have also revealed that the time-bandwidth products can be relatively near the minimum [19,34,35].

Another remarkable similarity of both lasers lies in the scaling of the pulse duration versus parameters Eqs. (11) and (13). Indeed, the minimum pulse duration t_L scales as the geometric average between the gain medium characteristic time t_U and the mode-locker characteristic time: the bunch duration t_b for free-electron lasers or the the modulator period T_m for the active mode locking. This geometric average scaling was noted from the beginning in the classical laser community [9], as well as in the FEL community [20,36].

As a consequence, typical visible-UV storage-ring free-electron lasers (for which $t_b \gg t_U$) emit pulses in the range of tens of picoseconds, although the gain medium has the capability to amplify much shorter pulses (e.g., in the range of 1 fs or hundreds of femtoseconds for super-ACO, UVSOR, and ELETTRA). This is exactly the same limitation that affected classical actively-mode-locked lasers.

In the case of FEL oscillators, the limit t_U could be attained in situations where the bunch duration was of the order of t_U (this corresponds to a situation where the bunch length is of the order of the slippage length). Up to now this was realized essentially in LINAC-based free-electron lasers [37].

VI. CONCLUSION

A complete analogy between of the temporal, spectrotemporal, and spatiotemporal dynamics of a storage-ring free-electron laser and an actively-mode-locked laser has been done. A full comparison of the models shows that the systems have similar Haus-like equations.

One common feature is the possibility of self-pulsing when the laser is detuned. This effect is strongly linked to the slow damping of the gain variable. It is the reason why this is observed in class-B lasers and storage-ring free-electron lasers.

Another common feature is the occurrence of a complex spatiotemporal evolution at very small detunings. In both free-electron lasers and classical lasers, this leads to an increase of spectrum width and pulse duration and prevents the actual observation of the calculated deterministic solution (supermodes [14,20] in the context of free-electron lasers). It is important to note that the use of a storage ring or a class-B operation in general is not necessary for this problem to occur. The main condition is that the characteristic time t_U (which is associated with gain and loss filtering over one cavity round-trip) be much smaller than the bunch duration. Once this condition is satisfied, small detunings are expected to induce the hypersensitivity to noise, which is widely studied in classical lasers [11–13].

A more efficient analogy of lasers and seeded FEL dynamics would certainly be helpful in the study of nonlinear optics and free-electron lasers. The time scales of storage-ring free-electron lasers allow observations of the mode-locking processes in a more direct way than in traditional mode-locked lasers. Conversely, dynamical issues in FEL oscillators may be anticipated from the knowledge of classical mode-locked lasers and generalization of the use of the Haus-type equations. For instance, knowledge from lasers motivates similar dynamical studies in the context of x-ray FEL oscillator projects [8].

ACKNOWLEDGMENTS

The CERLA is supported by the French Ministère chargée de la Recherche, the Région Nord-Pas de Calais and the Fonds de Développement Economique de Régions.

APPENDIX A: ASYMPTOTIC EXPANSIONS OF FREE-ELECTRON-LASER AND MODE-LOCKED-LASER EQUATIONS FOR THE FIELD

By making some assumptions, we demonstrate in the following that Eqs. (1) and (2) are similar except that a synchronous pump is not used. First, we suppose that in the vicinity of the laser pulse, the gain form can be approximated by an appropriate slow parabolic form: $f(\theta) = 1 - \epsilon^4\theta^2 + O(\epsilon^5)$. In addition, the pulse evolves on a lower time scale than θ because the typical width of the electron bunches is around 200 ps and that of the FEL pulse is around 10 ps. As a consequence, one has the change scale $Z = \epsilon\theta$. Under these approximations and using the Taylor approximation of order ϵ^2, Eq. (1) becomes

$$e_T(Z,T) = -[1 + g(T)\epsilon^2 Z^2]e(Z,T) + g(T)e(Z,T) - \epsilon v e_Z(Z,T) + g(T)\epsilon^2 e_{ZZ}(Z,T) + \sqrt{\eta}\xi. \tag{A1}$$

In this equation, in analogy to actively-mode-locked lasers, the losses are modulated in Z^2. The amplification comes only from the time-dependent gain. In contrast, the diffusion term now depends on the factor form, which, however, is not so relevant concerning the temporal and spectrotemporal dynamics. Another difference comes from the noise term. It is naturally present in Eq. (1) because the free-electron laser originates from the spontaneous emission of the electrons traveling through a periodic magnetic structure. Including a similar term in Eq. (2) is justified.

APPENDIX B: DERIVATION OF PULSE SHAPE AT ZERO DETUNING

In actively-loss-modulated lasers as well as storage-ring free-electron lasers, an usual situation is

$$\sigma_b \gg 1, \tag{B1}$$

$$\mu^{-1} \gg 1 \tag{B2}$$

for free-electron lasers and mode-locked lasers, respectively. In the FEL case, this corresponds to an electron bunch that is much longer that t_U (where t_U measures the duration of the shortest pulse that may amplify the medium and is of the order of the slippage duration). This is typically the case is storage-ring free-electron lasers (but not in LINAC-based FEL oscillators), where t_U is of the order of hundreds of femtoseconds. In mode-locked lasers, this is also frequent as the modulation period is usually long (in the nanosecond range) compared to t_U (in the picosecond or femtosecond range).

In this case, it is relatively easy to calculate an approximation of the pulse shape near zero detuning, where a stable solution is expected. Such calculations can be found in the literature for mode-locked lasers [9,11]. For free-electron lasers, attention has been focused on the pulse buildup (see, e.g., Ref. [36] for a study of the pulse shape and the spectrum versus time).

We present here the stationary states for Eqs. (1) and (7) for the case in which $\alpha = 0$, $v = 0$ (where shortest pulses are expected), and $\eta = 0$ because noise has little effect near zero detuning. In the case $\sigma_b \gg 1$, as seen in Appendix A, we can perform a Taylor expansion of $f(\theta)$ near its maximum. Moreover, when the stationary state is reached, i.e., $e_T(\theta,T) = 0$, the gain g is close to 1 and the stationary solution $e_S(\theta)$ is a slowly varying function. This motivates the following expansion:

$$Z = \epsilon\theta, \tag{B3}$$

$$\epsilon^4 = 1/2\sigma_b^2, \tag{B4}$$

$$f(\theta) = 1 - \epsilon^2 Z^2 + O(\epsilon^4), \tag{B5}$$

$$g = g_0 + \epsilon^2 g_2 + O(\epsilon^4), \tag{B6}$$

$$e_S(\theta) = E_0(Z) + \epsilon^2 E_2(Z) + O(\epsilon^4). \tag{B7}$$

Substituting in Eq. (1), we obtain

$$-E_0(Z) - \epsilon^2 E_2(Z) + g_0[E_0(Z) + \epsilon^2 E_{0ZZ}(Z) + \epsilon^2 E_2(Z)] - \epsilon^2 g_0 Z^2 E_0(Z) + \epsilon^2 g_2 E_0(Z) + O(\epsilon^4) = 0. \tag{B8}$$

Up to order ϵ^2, we have

$$-E_0(Z) + g_0 E_0(Z) = 0, \tag{B9}$$

$$E_2(Z) - g_0 E_2(Z) = g_0 E_{0ZZ}(Z) - g_0 Z^2 E_0(Z) + g_2 E_0(Z). \tag{B10}$$

This leads to

$$g_0 = 1, \tag{B11}$$

$$E_{0ZZ}(Z) - Z^2 E_0(Z) + g_2 E_0(Z) = 0. \tag{B12}$$

The solutions for $E_0(Z)$ are Hermite-Gauss functions. Only the fundamental one is expected to be stable at $v = 0$ [11]. It is easy to show that this solution can be written

$$g_2 = 1, \tag{B13}$$

$$E_0(Z) = ae^{-Z^2/2}, \tag{B14}$$

with a a parameter that will not be determined here. Hence, using the original variables, the stationary solution can be written

$$e_S(\theta) \approx ae^{-\theta^2/4\sigma_L^2}, \tag{B15}$$

with the rms laser pulse width σ_L being defined by

$$\sigma_L = 2^{-1/4}\sqrt{\sigma_b}. \tag{B16}$$

At this step, it is worth expressing the laser pulse shape as a function of physical time t (in seconds):

$$e_S(t) = ae^{-t^2/4t_L^2}, \tag{B17}$$

with $t_L = 2^{-1/4}\sqrt{t_b t_U}$ and t_b representing the rms bunch duration (in seconds). It is also remarkable that the Gaussian shape is similar for the FEL startup as well (called supermodes in FEL theory), as was shown in several studies [20,36].

[1] J. M. J. Madey, J. Appl. Phys. **42**, 1906 (1971).

[2] D. A. G. Deacon, L. R. Elias, J. M. J. Madey, G. J. Ramian, H. A. Schwettman, and T. I. Smith, Phys. Rev. Lett. **38**, 892 (1977).

[3] M. Billardon, P. Elleaume, J. M. Ortega, C. Bazin, M. Bergher, M. Velghe, Y. Petroff, D. A. G. Deacon, K. E. Robinson, and J. M. J. Madey, Phys. Rev. Lett. **51**, 1652 (1983).

[4] S. Koda, M. Hosaka, J. Yamazaki, M. Katoh, and H. Hama, Nucl. Instrum. Methods Phys. Res. A **475**, 211 (2001).

[5] G. De Ninno, A. Antoniazzi, B. Diviacco, D. Fanelli, L. Giannessi, R. Meucci, and M. Trovó, Phys. Rev. E **71**, 066504 (2005).

[6] S. Bielawski, C. Szwaj, C. Bruni, D. Garzella, G. L. Orlandi, and M. E. Couprie, Phys. Rev. Lett. **95**, 034801 (2005).

[7] Y. K. Wu, N. A. Vinokurov, S. Mikhailov, J. Li, and V. Popov, Phys. Rev. Lett. **96**, 224801 (2006).

[8] K.-J. Kim, Y. Shvyd'ko, and S. Reiche, Phys. Rev. Lett. **100**, 244802 (2008).

[9] H. A. Haus, IEEE J. Sel. Top. Quantum Electron. **6**, 1173 (2000).
[10] C. Evain, C. Szwaj, S. Bielawski, M. Hosaka, M. H. A. Mochihashi, M. Katoh, and M.-E. Couprie, Phys. Rev. Lett. **102**, 134501 (2009).
[11] J. B. Geddes, W. J. Firth, and K. Black, SIAM J. Appl. Dyn. Syst. **2**, 647 (2003).
[12] U. Morgner and F. Mitschke, Phys. Rev. E **58**, 187 (1998).
[13] F. X. Kärtner, D. M. Zumbühl, and N. Matuschek, Phys. Rev. Lett. **82**, 4428 (1999).
[14] G. Dattoli, T. Hermsen, A. Renieri, A. Torre, and J. C. Gallardo, Phys. Rev. A **37**, 4326 (1988).
[15] T. Kolokolnikov, M. Nizette, T. Erneux, N. Joly, and S. Bielawski, Physica D **219**, 13 (2006).
[16] P. Ellaume, IEEE J. Quantum Electron. **21**, 1012 (1985).
[17] P. Elleaume, J. Phys. (Paris) Colloq. **44**, C1-353 (1983).
[18] M. Hosaka, M. Katoh, A. Mochihashi, J. Yamazaki, K. Hayashi, and Y. Takashima, Nucl. Instrum. Methods Phys. Res. A **528**, 291 (2004).
[19] R. P. Walker *et al.*, Nucl. Instrum. Methods Phys. Res. A **475**, 20 (2001).
[20] G. Dattoli, T. Hermsen, L. Mezi, A. Renieri, and A. Torre, Phys. Rev. A **37**, 4334 (1988).
[21] P. Elleaume, Nucl. Instrum. Methods Phys. Res. A **237**, 28 (1985).
[22] R. Bonifacio, C. Pellegrini, and L. M. Narducci, Opt. Commun. **50**, 373 (1984).
[23] A. E. Siegman, *Lasers* (University Science Books, Sausalito, CA, 1990).
[24] G. D. Ninno, D. Fanelli, C. Bruni, and M. E. Couprie, Eur. Phys. J. D **22**, 269 (2003).
[25] R. L. Honeycutt, Phys. Rev. A **45**, 600 (1992).
[26] M. Frigo and S. G. Johnson, Proc. IEEE **93**, 216 (2005), http://www.fftw.org/.
[27] V. N. Litvinenko, S. H. Park, I. V. Pinayev, and Y. Wu, Nucl. Instrum. Methods Phys. Res. A **475**, 240 (2001).
[28] C. Bruni, S. Bielawski, G. L. Orlandi, D. Garzella, and M. E. Couprie, Eur. Phys. J. D **39** 75 (2006).
[29] P. Wang *et al.*, in *Status Report on the Duke FEL Facility*, Proceedings of the 2001 Particle Accelerator Conference, Chicago, edited by P. Lucas and S. Webber (IEEE, Piscataway, NJ, 2001), p. 2819.
[30] G. D. Ninno *et al.*, Nucl. Instrum. Methods Phys. Res. A **507**, 274 (2003).
[31] K. Yamada, N. Sei, M. Yasumoto, H. Ogawa, T. Mikado, and H. Ohgaki, Nucl. Instrum. Methods Phys. Res. A **483**, 162 (2002).
[32] R. Roux, M. E. Couprie, R. J. Bakker, D. Garzella, D. Nutarelli, L. Nahon, and M. Billardon, Phys. Rev. E **58**, 6584 (1998).
[33] M. Hosaka, S. Koda, J. Yamazaki, and H. Hama, Nucl. Instrum. Methods Phys. Res. A **445**, 208 (2000).
[34] M. E. Couprie, G. D. Ninno, G. Moneron, D. Nutarelli, M. Hirsch, D. Garzella, E. Renault, R. Roux, and C. A. Thomas, Nucl. Instrum. Methods Phys. Res. A **475**, 229 (2001).
[35] V. N. Litvinenko, S. H. Park, I. V. Pinayev, Y. Wu, A. Lumpkin, and B. Yang, Nucl. Instrum. Methods Phys. Res. A **475**, 234 (2001).
[36] K.-J. Kim, Phys. Rev. Lett. **66**, 2746 (1991).
[37] R. Prazeres, J. M. Berset, F. Glotin, D. A. Jaroszynski, and J. M. Ortega, Nucl. Instrum. Methods Phys. Res. A **358**, 212 (1995).